Journal of Aeronautics, Astronautics and Aviation, Vol. 58, No. 6S, pp. 799 – 810 (2026)
https://doi.org/10.6125/JoAAA.202606_58(6S).06

Effect of Multi-Walled Carbon Nanotubes on the Mechanical Properties of Carbon Resin and Carbon-Fibre Reinforced Polymer

Najihah Mohd Tamyis [1 *], John Patrick A. Fairclough [2], Mohd Roshdi Hassan [3], Harlisya Harun [1]

[1] *Universiti Kuala Lumpur Malaysia Institute of Aviation Technology, Dengkil, 43900 Selangor, Malaysia.*
[2] *Department of Mechanical Engineering, University of Sheffield, Sheffield S3 7HQ, UK.*
[3] *Department of Mechanical and Manufacturing Engineering, Universiti Putra Malaysia, 43400 Serdang, Selangor, Malaysia.*

ABSTRACT

This study investigated the incorporation of two lengths of multi-walled carbon nanotube (MWCNT), i.e., MWCNT_long (length 10 - 30 μm) and MWCNT_short (length 0.5 - 2.0 μm), into epoxy resins and the use of a combination of three methods for dispersing the MWCNT into Epikote 828 epoxy resin. The MWCNTs were first mixed with the epoxy resin using a high-shear mixer, sonicated, and finally calendared by a three-roll mill with 4, 4-diaminodiphenyl sulfone as the hardener. The fractograph of the flexural-fractured surface showed a significant difference in the fracture surfaces. The epoxy resin containing MWCNT showed an enhanced roughness in the fractured surface compared to the epoxy resin without MWCNT, which had a plain and featureless appearance. Adding 0.38% of MWCNT_short improved the interlaminar shear strength (ILSS) by 14%. However, adding MWCNT_long reduced ILSS by 17.9%. This is because MWCNT_long's intensity ratio through Raman Spectroscopy, was higher than that of MWCNT_short, with values of 0.68 and 0.39, respectively. This suggests that MWCNT_long has a higher concentration of carbon atom defects, which reduces the quality of the nano-modified resin.

Keywords: Carbon fibre composites, Epoxy, Fractograph, Interlaminar shear strength, Multi-walled carbon nanotubes

I. INTRODUCTION

With the ever-increasing concern and more stringent legislative regulation over carbon emissions, manufacturers of automobile and aerospace crafts are now seriously looking into reducing the emissions of the vehicles that they produce. One of the strategies for lowering carbon emission is to reduce the weight of the vehicles [1-3]. This "light-weighting" is particularly important for aircraft, city, and performance cars because it can increase energy efficiency and performance by lowering the mass that must be propelled, thereby decreasing fuel consumption, reducing emissions, and improving dynamic responsiveness. In this respect, the carbon-fibre-reinforced polymer (CFRP) has now been commonly used in the aerospace and high-end automobile manufacturing sector because of the extraordinary strength and stiffness of its carbon-fibre composites.

However, if loads are not adequately applied to the fibre's axis, the stress would be exerted on its resin matrix. Consequently, the mechanical properties of the fibre in terms of flexure, twisting, and off-axis loading would then strongly depend on the polymer resin matrix. Usually, the deteriorated modes encompass matrix splintering, interfacial detachment between the fibre and the matrix, and interlaminar delamination. A promising technique in reducing this deterioration or failure is to reinforce the composite with nanoparticles that possess superior mechanical, thermal, and electrical attributes, such as the carbon nanotubes (CNTs) [1-3]. By way of comparison,

Manuscript received, October 9, 2025, final revision, February 26, 2026
* To whom correspondence should be addressed, E-mail: najihah@unikl.edu.my

the modulus elasticity and tensile strength of CNT range from 250 - 1200 GPa and 10 - 200 GPa, respectively, which are more superior to that of carbon fibres at 230 - 445 GPa and 3 – 6 GPa, respectively [4,5].

The epoxy resin would show markedly enhanced attributes if CNTs are well dispersed in it [6,7]. However, dispersing CNT in a resin matrix is a formidable task, since CNTs are commercially produced as powders packed into intertwined sheaves [1]. Also, CNTs are non-polar, chemically stable, and inert with limited solubility [9]; they only weakly interact with other materials through van der Waals interactions [1,8]. However, Van der Waals interactions within the CNT are generally higher than that with the epoxy resin, thus rendering the dispersion of CNTs into polymeric matrices highly challenging [1,9].

For a uniform dispersion, the sheaves of CNT will need to be disentangled without breaking for maximal contact with the epoxy matrix. Owing to deficient dispersion, the presence of CNT agglomerates within a resin nanocomposite would fracture, thereby reducing the robustness and toughness of the resin and composites [10,11]. Thus, reinforcing composites with nanomaterials might be weakening, instead of strengthening, their mechanical attributes because the extent of reinforcement is largely dependent on how well the distribution of the nanomaterials is.

Several techniques such as mechanical mixing, high-shear mixing, ultrasonication, and calendaring (alias three-roll milling) are known for dispersing CNTs [2,12,13]. Among them, ultrasonication is the most widely used method for dispersing CNTs in epoxy resins as it could shorten the CNT length besides disaggregating the sheaves[14–16]. Indeed, high sonication energies (85 kJ) could effectively shorten the CNT length, thereby reducing its aspect ratio (length/diameter) [17] for a more efficient dispersion. In contrast, a high aspect ratio of CNT strengthens the mechanical attributes of the fortified composites and inhibits dispersion [10,17].

Although ultrasonication alone can disperse CNT in the epoxy resin, it is generally used together with other methods [18]. For a full dispersion, CNT will need to be separated from the agglomerates via high-shear mixing for as far as 24 hours [19], but this extended blending may break the multi-walled carbon nanotube (MWCNT), thereby diminishing the nanocomposites' mechanical features [19,20]. Meanwhile, although calendaring does not segment the CNT [21], this method generates a homogenous dispersion [1,12,22,44]. During the calendaring, the nanocomposite mixture is moved through a series of cylinders that revolve at different velocities or rollers with a user-defined space typically ranging from 1 - 5 μm between two adjacent cylinders. If this space is much larger than the CNT radius of gyration, the dispersion process will be ineffective. This indicate that calendaring is more effectively disperse the big agglomerated CNTs into little ones at the sub-micron level [1]. Consequently, the method of three-roll milling is suitable for high-volume production of nanocomposites, especially it could be easily configured from the laboratory scale to mass production and hence cost-effective [22].

This study investigated the effectiveness of dispersing CNTs in epoxy resins via a combination of three mechanical techniques, i.e., high-shear mixing, ultrasonication, and three-roll milling, over a short period to disperse MWCNT. This study might facilitate the production of a uniform distribution of MWCNT within an epoxy matrix system while shortening the duration for maneuvering the composites. Furthermore, the nano-modified composites produced in this work were successfully fabricated using three mixing approaches, high-shear mixing (10 min), ultrasonic probing (15 min), and three-roll milling (15 min). The principal novelty of this study is the demonstration that a high-quality dispersion of CNTs can be accomplished within a markedly short processing time, highlighting a rapid and practical method for scalable composite manufacturing.

II. EXPERIMENTAL DETAILS

2.1 Materials

In this study, the resin matrix for the composites comprised the epoxy resin of bisphenol A and epichlorohydrin, commercially known as Epikote 828, and the hardener 4, 4-diaminodiphenyl sulfone (DDS). Both chemicals were purchased from Sigma Aldrich. Together, these chemicals would provide the intermolecular intertwining to generate a tough thermosetting system. Meanwhile, the MWCNTs, designated as 1236YJS (0.5 2.0 μm in length) and 1205YJ (10 - 30 μm in length) with diameters in the same range, i.e., 10 - 20 nm externally and 5 - 10 nm inwardly, were procured from Nanostructured and Amorphous Materials, Inc. USA at a quoted purity of 95%. These MWCNTs were manufactured via the catalytic chemical vapour deposition (CVD) and the plain fabricate of T300 carbon fibre (Easycomposites.com) was employed to reinforce the composites.

2.2 Fabrication of MWCNT resin

The MWCNT-free or neat epoxy resin served as the control study, which consisted of 100 parts of Epikote 828 cured with 30 per hundred of resin (phr) DDS by weight . The mixture was stirred with an overhead agitator in a boiling oil bath at 140°C for 10 - 15 min, and the entrapped air was removed in a vacuum oven at 120 °C for 10 - 15 min.

In this study, two batches of composites were prepared from MWCNT, namely, 1205YJ (tagged as MWCNT_long/828) and 1236YJS (tagged as MWCNT_short/828). Figure 1 illustrates the fabrication of MWCNT/828 nanocomposites, in which MWCNT was first dispersed manually by mingling Epikote 828 with 0.5% MWCNT (by weight). The mixture was then blended in a high-shear mixer (L2R, Silverson) to break those larger agglomerates into smaller agglomerates. A sonicator (200s Hielscher UP, 200 watts, 24 kHz) with a Sonotrode S7 probe and a tip diameter of 22 mm was used to sonicate the MWCNT/Epikote 828 mixture into smaller parts [23] for 15 min at a submersion depth of 3.5 cm from the mixture surface for the Sonotrode. The probe was inserted at the centre of a 400-mL beaker that contained the mixture. The beaker containing the mixture was placed in a water

bath during the 15-minute dispersion and a 15-second cycle of ON/OFF was set to lower the temperature increment generated by the sonication.

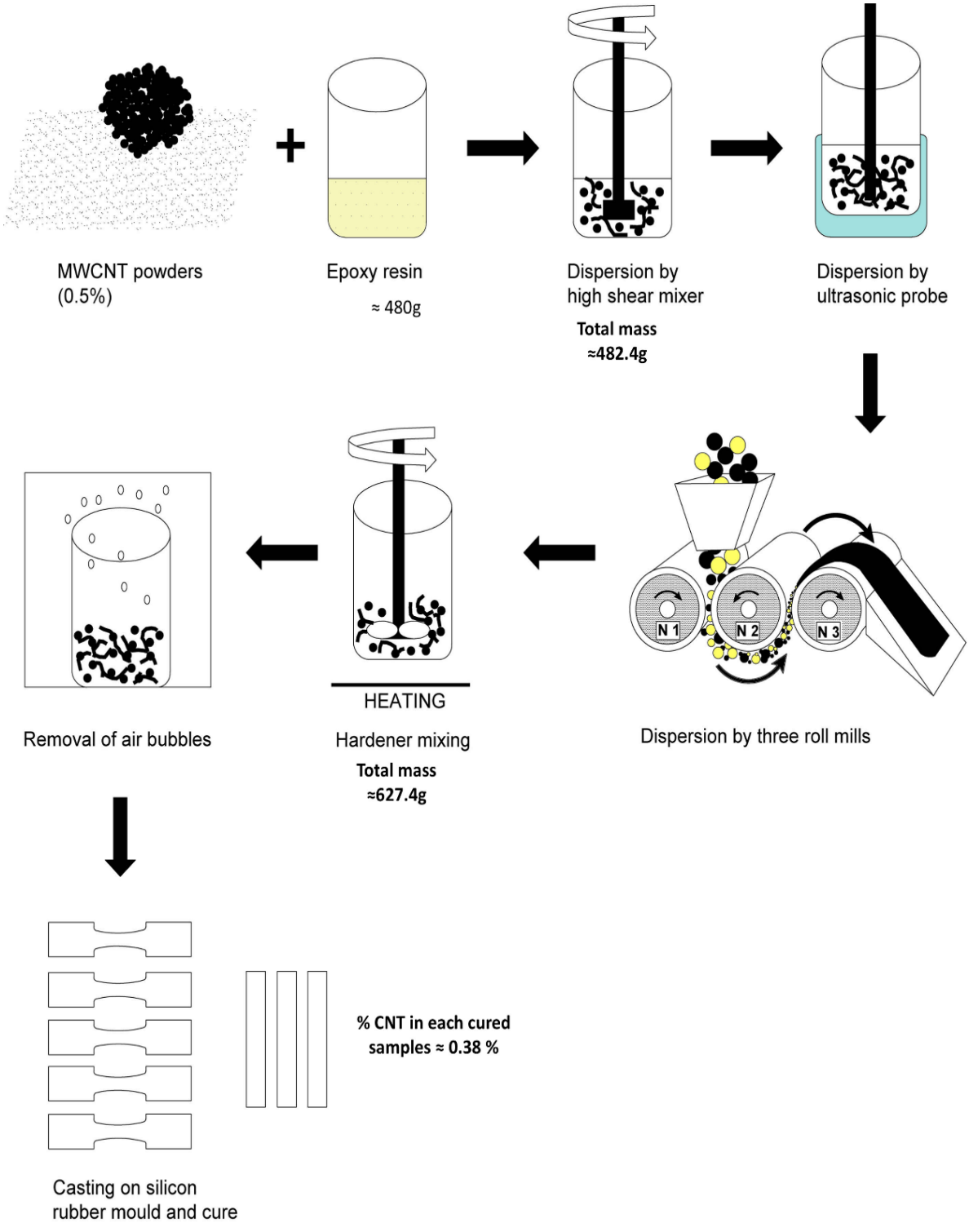

Figure 1 The fabrication of MWCNT/828 nanocomposites.

The last step of dispersing MWCNT into Epikote 828 comprised blending by calendaring with a three-roll mill (80E, Exakt) with a diameter of 80 mm and 200 mm in width. The rollers' revolving speed varied from 200 to 300 rpm but the ratio of their angular velocities was riveted ($\omega_{1(\text{feed roll})}$: $\omega_{2\ (\text{central roll})}$: $\omega_{3(\text{apron roll})}$ = 1: 3: 9) [24–26]. Roller by pass: 1st pass, speed (rpm) 200. 2nd pass, speed rpm 300. 3rd pass speed rpm 300. In the three-roll mills method, the number of passes can be decreased and therefore the time of dispersion can be reduced. The feed roll revolved

alongside the apron roll while the central roll gyrated in the opposite direction. Unequal angular velocities produced shear that induced the mixing of MWCNT into Epikote 828. The rollers were kept between 20 and 25 °C to circumvent heating the resin, thereby lowering the viscosity while decreasing the stress transfer. Upon completing the dispersion, the MWCNT/Epikote828 mixture was blended by an overhead stirrer with the DDS curing agent. Finally, all the resin systems, with and without MWCNT, were cured at 120 ℃ for 2 h, then post-cured at 185 ℃ for 6 h at a ramp rate of 2 ℃/min, and cooled to room temperature at 2 ℃/min. The calculated final proportion of MWCNT in each cured nanocomposite sample was 0.38%.

2.3. Fabrication of carbon-fibre-reinforced (CFRP) composites laminates

Resin impregnation was performed manually with 16 layers of plain weave T300 carbon fibre fabric cut into 250 mm x 350 mm rectangles. Figure 2 shows the setup for the impregnation of resin, and the hotplate was adjusted to 80 °C to reduce the viscosity of the resin for percolating into the fabric. The resin was consolidated into the carbon fibre with a plastic applicator, placed in a beaker, and immersed into an oil bath at 80 °C intermittently for 3 mins. This process was performed as rapidly as possible to hinder the resin molecule from crosslinking.

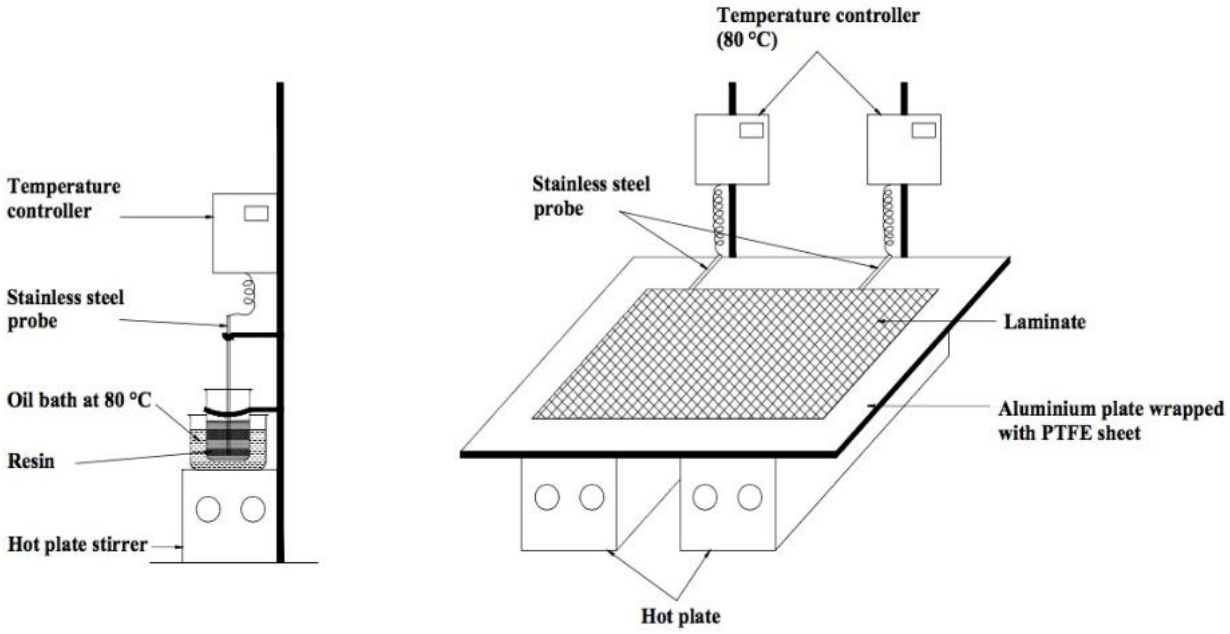

Figure 2 Setup for CFRP

III. CHARACTERISATION

3.1 Characterisation of MWCNT

Figure 3 shows the Raman spectra of MWCNT with distinctive peaks at 1577 cm^{-1} (G-band) and 1340 cm^{-1} (D-band) for MWCNT_long/828/DDS, peaks at 1616 cm^{-1} (G-band) and 1325 cm^{-1} (D-band) for MWCNT_short/828/DDS. The ratio of D-band to G-band (I_D/I_G), commonly known as intensity ratio, R, measured the integrity of the dispersed MWCNT [27,28]. Given that a low I_D/I_G was indicative that sp^2 bonded carbon atoms have relatively pure with little foreign matter or defects, while a high I_D/I_G ratio would indicate the presence of a substantial amount of impurities or defects in the samples. Table 1 summarises the findings of Raman analysis with an I_D/I_G ratio 0.68 for MWCNT_long/828/DDS and 0.39 for MWCNT_short/828/DDS. In general, the increment of the I_D/I_G ratio value was proportional to the amount of 'unorganised' carbon but inversely related to the decrease in the mean crystal size [29, 30].

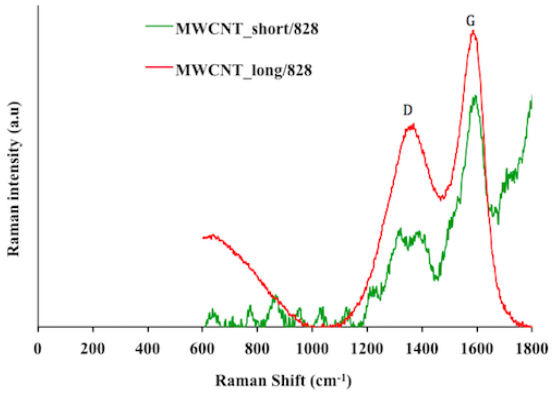

Figure 3 Raman Spectra of MWCNT_long/828 and MWCNT_short/828

Table 1 A Summary of Results from Raman Spectra

	Raman shift (cm^{-1})		Intensity		R
Samples	X_D*	X_G	I_D	I_G	I_D/I_G
MWCNT_long	1340	1577	427	627	0.68
MWCNT_short	1325	1616	200	501	0.39

3.2 Characterisation of the Dispersion

The dispersion of MWCNT in Epikote 828/DDS resin was evaluated using transmission electron microscopy (TEM). Samples of cured resin, sliced to a thickness of 80 nm, were examined using a Transmission Electron Microscope (G^2 FEI Tecnai) with an escalating voltage of 80 kV. The MWCNT_long dispersed more uniformly than the MWCNT_short nonomodified resin. Figure 4(a) shows that MWCNT_long was evenly spaced. However, the length of the MWCNT was on average less than 500 nm. Quantifying the actual length via TEM was a challenging task because the sections were merely 80 nm in thickness and the MWCNT resin would inevitably be minced during the sectioning. The MWCNT_long of Figure 4(b) was 1.4 μm in length; MWCNTs that were in parallel with the cutting axis remained intact. Although the MWCNT_short resin appeared to be well dispersed (Figure 5(a)), they showed areas of even MWCNT density with some visible agglomerated zones (Figure 5(b)).

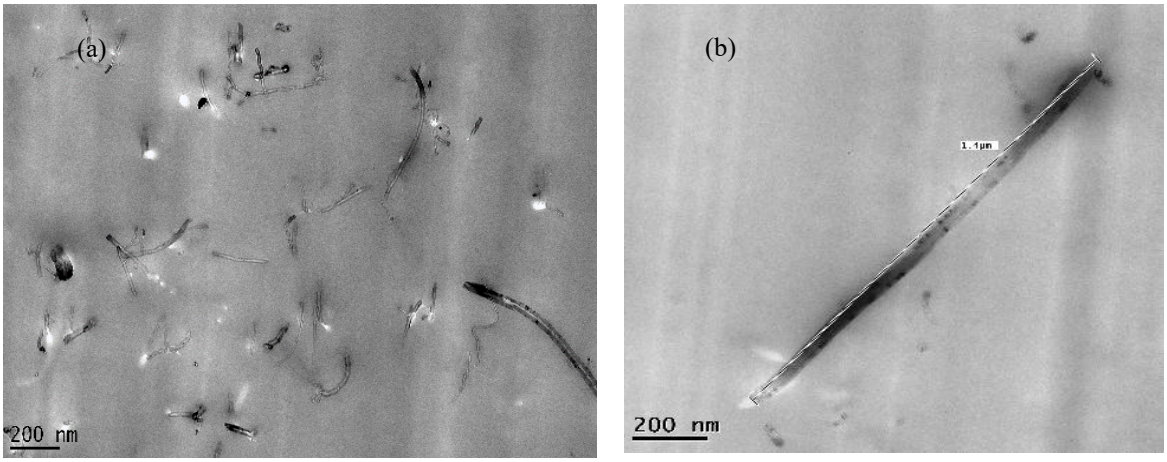

Figure 4 TEM images of the MWCNT_long/Epikote 828: (a) the dispersion of MWCNT_long/Epikote 828, (b) a single strand of the MWCNT_long after the dispersion with the length of 1.4 μm

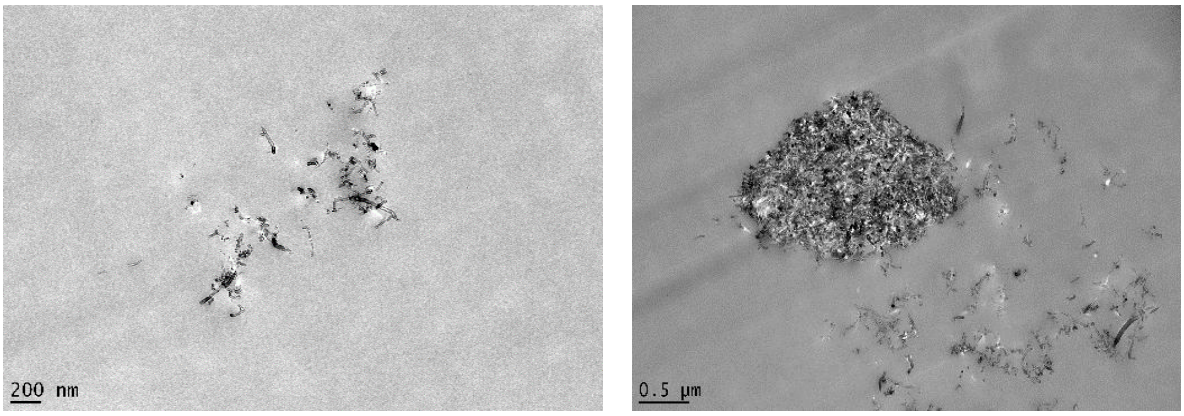

Figure 5 (a) The dispersion of MWNCT_short in the epoxy resin matrix, (b) An agglomerate on a scale bar 0.5 μm for the MWCNT_short/828 after the complete mixing using the combination of the three methods

IV. MECHANICAL ANALYSIS

4.1 Compression and flexural tests for the epoxy polymer

The static unaxial compression tests were performed on cylindrical samples of epoxy resin. The cylindrical shaped were made with a height of 10mm and a diameter of 10mm (1:1 dimension ratio). Compressive attributes such as elastic modulus, failure, yield strength, and strain at the yield point, were assessed following the standards of British's National Standard, European Standard and International Organization for Standardization (BS EN

ISO) 604:2003 [31] and the American Society for Testing and Materials (ASTM) D695 [32]. The compressive modulus (E) was computed at 2 to 3% of the strain. Table 2 compares the compressive characteristics of neat resin, MWCNT_long/828/DDS, and MWCNT_short/828/DDS. The compressive strength and stress at break (σ_B) for both MWCNT/828/DDS systems were substantially greater than that of the neat resin. In contrast, the E value of the neat 828/DDS was slightly larger than that of MWCNT_long/828/DDS but slightly lower than that of MWCNT_short/828/DDS. The neat resin showed the highest value for compressive strain (ε_y) and stress (σ_y) at the yield point, i.e., 13.24 ± 0.66, and 155.34 ± 1.92, respectively. Table 2 suggests that the nanocomposites become more brittle while simultaneously increasing its strength in comparison to the neat epoxy with the addition of MWCNTs.

Meanwhile, flexural properties such as flexural strength, failure strain, and flexural were determined according to the standard of BS ISO 178:2010. Rectangular samples of cured resins with 70 mm length, 10 mm width and 4 mm thickness were used for the flexural test. Table 3 shows that the flexural strength for both nanocomposite systems increased by 4.1 - 4.7% compared to the neat resin.

Table 2 The compressive attributes of Epikote 828+DDS epoxy resin, MWCNT_long/828 epoxy resin, and MWCNT_short epoxy resins generated from cylindrical samples of 10 mm diameter x 10 mm length with six replicates for each system

Compressive attributes	Sample type		
	Neat Resin Epikote 828/DDS	MWCNT_long/ 828/DDS	MWCNT_short/ 828/DDS
Stress at break(MPa)	315.66 ± 2.90	330.73 ± 5.20	340.86 ± 5.48
Strain at break (%)	42.33 ± 0.97	49.12 ± 0.03	51.32 ± 0.78
Modulus (GPa)	1.61 ± 0.12	1.56 ± 0.07	1.72 ± 0.08
Stress at yield point (MPa)	155.34 ± 1.92	140.72 ± 0.27	140.27 ± 0.33
Strain at yield point (%)	13.24 ± 0.66	12.56 ± 0.50	12.47 ± 0.58

Table 3 The flexural properties of Epikote 828/DDS resin, MWCNT_long/828/DDS, and MWCNT_short/828/DDS resins evaluated via a three-point bending test with six replicates for each system

	Neat Resin Epikote 828/DDS	MWCNT_ long/828/DDS	MWCNT_short/828/DDS
Flexural modulus (GPa)	2.45 ± 0.10	2.72 ± 0.09	2.88 ± 0.07
Flexural strength (MPa)	136.19 ± 6.44	141.71 ± 5.78	142.61 ± 3.09
Failure strain (%)	6.89 ± 0.53	7.11 ± 0.51	6.92 ± 0.26

4.2 Interlaminar shear stress (ILSS) of CFRP composites

If a horizontal shear load on laminates surpasses the ILSS, then delamination of layers would ensue. The ILSS of a laminate composite could be quantified by generating a pure ILSS to instigate a failure [33]. Based on the classical beam theory (Bernoulli-Eular), the ILSS of the CFRP composites (30 mm x 8 mm x 4.5 mm in dimension) was quantified using the short-beam shear stress (SBS) test following the ASTM D2344 standard [34] and evaluated on a three-point bend test rig (Figure 6). The first failure, recorded as the horizontal load increased, was used to estimate the apparent interlaminar shear strength or short beam strength (F_{sbs}) of the composite, which was computed from Equation 1 [34].

$$F_{sbs} = 0.75 \frac{P_{max}}{w \, t} \quad (1)$$

where P_{max} = the maximum load, w = the width of the samples, and t = the thickness of the samples.

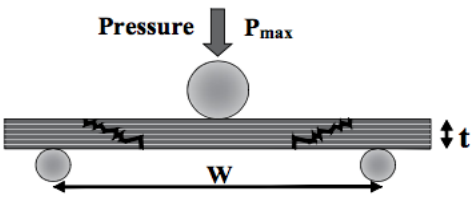

Figure 6 A schematic diagram of the short-beam shear (SBS)

Various mechanisms had been reported to impair the samples before or during the interlaminar shear failure [35-38]. In this study, the non-planar interlaminar region of reinforcement material (i.e., the plain weave carbon fibre), together with the matrix, would subject the sample to a range of other failure modes before the occurrence of shear failure due to the SBS loading. In spite of this constraint, the samples showed the typical behaviour of SBS strength-deformation. Figure 8 shows the plots of loads versus deflection for MWCNT_long/828/DDS carbon fibre and it exhibited similar behaviour as the neat resin carbon fibre/828/DDS (Figure 7). Overall, the curves increased to the maximal before slowly declining after the onset of cracking. This behaviour was more prominent in MWCNT_long/828/DDS samples.

Meanwhile, Figure 9 shows the plots of load versus deflection for the MWCNT_short/828/DDS composites. Curves increased proportionally with the deflection until the occurrence of a sudden decline, which indicated a distinctive catastrophic failure. This drastic decline of at least 30% of the peaked load was interpreted as a pure laminar shear failure [35,39]. These behavioural variations were attributable to different matrix characteristics, namely, a brittle matrix in MWCNT_short/ 828/carbon fibre CFRP composites (Figure 9) and a more ductile matrix in the MWCNT_long/ 828/carbon fibre CFRP composites (Figure 8) [39].

Apart from the interlaminar shear failure, other forms of failure would also cause these plots to behave differently. Analyses on ILSS graphs with different plots [35] indicated that samples producing curves similar to that of Figure 9 had experienced an interlaminar shear failure. In contrast, samples producing curves similar to that of Figure 10 were found to contain micro-cracking within the resin of the fibre tows, which was due to failures in compression and indentation at the loading point.

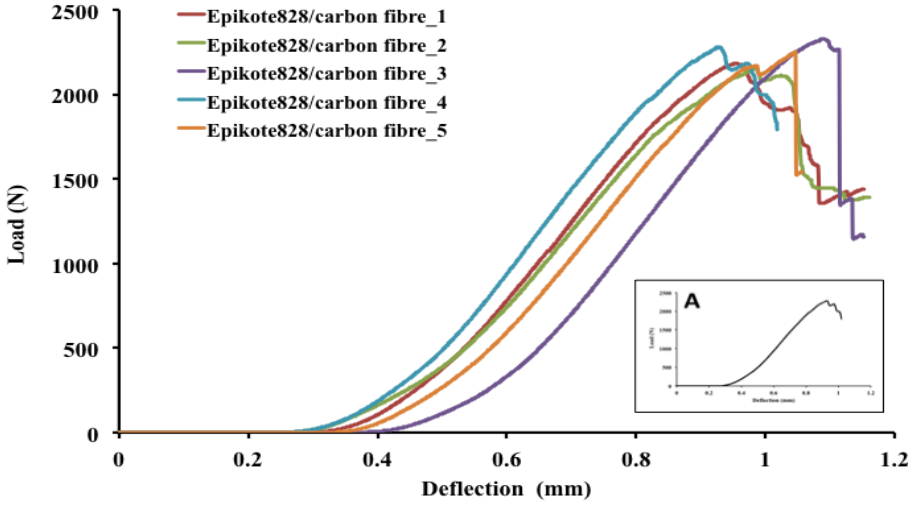

Figure 7 Plots of load vs. deflection for a short-beam shear on Epikote828/carbon fibre CFRP composites. The insert shows the average curve pattern for all samples

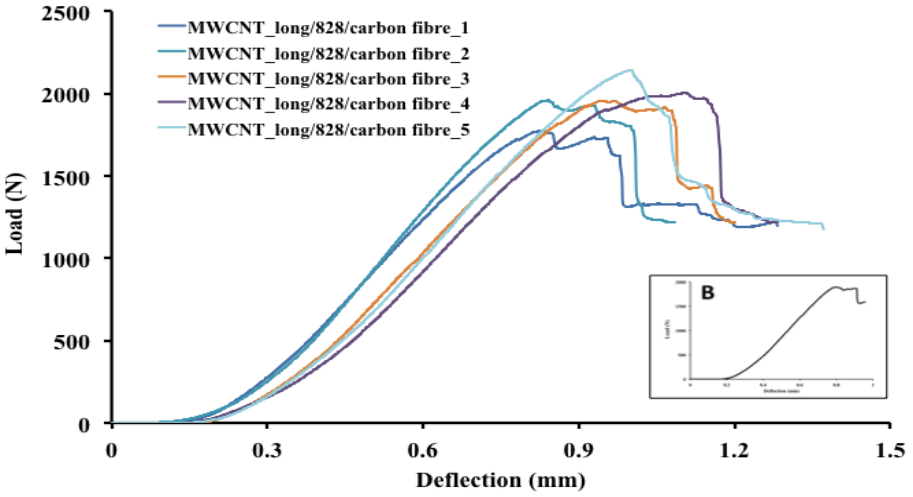

Figure 8 Plots of load vs. deflection for a short-beam shear on MWCNT_long/ 828/carbon fibre CFRP composites. The insert shows the average curve pattern for all samples

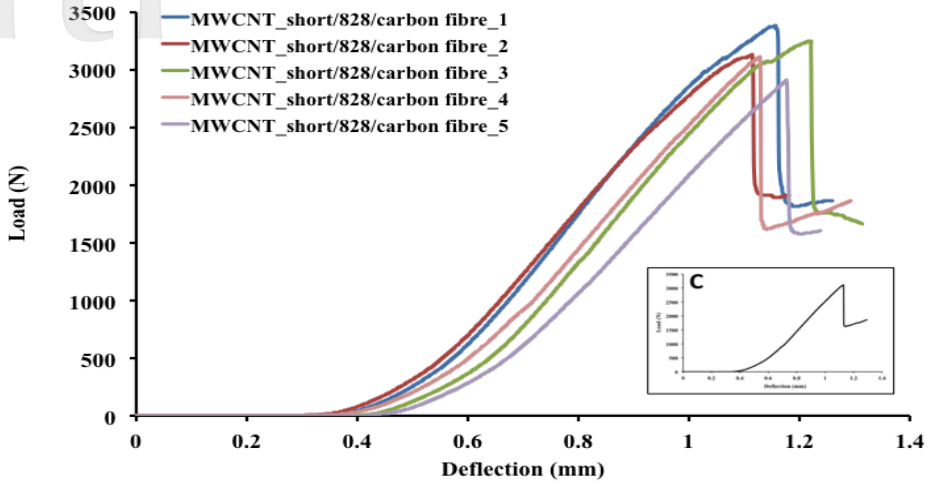

Figure 9 Plots of load vs. deflection for a short-beam shear on MWCNT_short/ 828/carbon fibre CFRP composites. The insert shows the average curve pattern for all samples

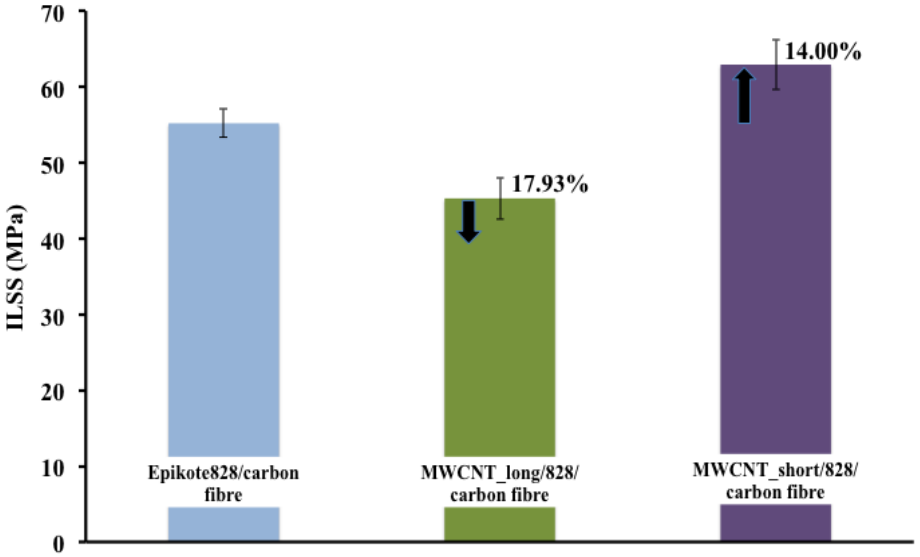

Figure 10 ILSS values for Epikote828/carbon fibre, MWCNT_long/828/carbon fibre and MWCNT_short/828/carbon fibre estimated with the SBS method

The relatively more ductile characteristic shown in Figure 8 was probably attributable to the bow out of the long MWCNT, suggesting that the van der Waal interaction at the interface of matrix-MWCNT was weak in the MWCNT_long/828/DDS samples. The variations in behavioral patterns (ductile vs. brittle) are attributed to different matrix characteristics influenced by the filler length [35,39]. The idea of a weakened interface in long MWCNTs by noting they have a higher concentration of carbon atom defects (indicated by a Raman ID/IG ratio of 0.68 compared to 0.39 for short MWCNTs). These defects are believed to reduce the quality of the nano-modified resin and contribute to the observed reduction in interlaminar shear strength (ILSS). Bowing out describes the physical deflection of long nanotubes made possible by poor interfacial adhesion (weak van der Waals forces), which grants the composite a degree of ductility at the expense of overall shear strength [15].

Table 4 shows the ILSS values of three resin systems, and the average ILSS value of the neat resin 828/DDS, MWCNT_long/828/DDS, and MWCNT_short/828/DDS CFRP composites were 55.2 ± 1.8, 45.3 ± 3.1, and 62.9 ± 3.7 MPa, respectively. Overall, the ILSS value of MWCNT_long/828/DDS carbon fibre was 17.9% lower than that of the neat resin Epikote 828/DDS carbon fibre as shown in Figure 10. However, the ILSS value of MWCNT_short/828/DDS carbon fibre soared by 14%. The standard deviation or sample's coefficient of variation ranged from 3.3 – 6.8% for each sample group. Statistical differences among sample groups were assessed with the analysis of variance (ANOVA) using the software Statistical Package for Social Sciences (version 20, IBM)

at the significance level of p-value which is less than 0.05. The presence of MWCNT significantly (p = 3 x 10^{-6}) impacted the ILSS of the CFRP composites.

Table 4 ILSS values for Epikote828/carbon fibre, MWCNT_long/828/carbon fibre, and MWCNT_short/828/carbon fibre estimated with the SBS method

Sample number	ILSS (MPa)		
	Epikote828/carbon fibre	MWCNT_long/828/ carbon fibre	MWCNT_short/828/carbon fibre
1	54.95	42.00	67.55
2	52.58	45.36	64.55
3	57.66	45.61	64.21
4	55.87	43.40	59.93
5	54.87	50.09	58.36
Average	55.19	45.29	62.92
Standard deviation	1.84	3.06	3.72
Coefficient of variation (%)	3.33	6.76	5.91
p-value	3 x 10^{-6}		

4.3 Characterisation of the Flexural-fractured Surface

Flexural-fractured surfaces of the Epikote 828/DDS and MWCNT/828/DDS systems were assessed by a Scanning Electronic Microscope (Tescan Vega3 LMU) with specimens mounted on aluminium stubs using sticky tabs and coated with a thin layer of gold using a coater (Edwards S150B Sputter). Figure 11 shows the neat Epikote 828 epoxy resin with a relatively even flexural-fractured surface, i.e., a typical fractography of brittle fracture behaviour, which was indicative of low fracture toughness. The two cleavage steps were separated by 100 – 200 μm with a relatively featureless cleavage plane.

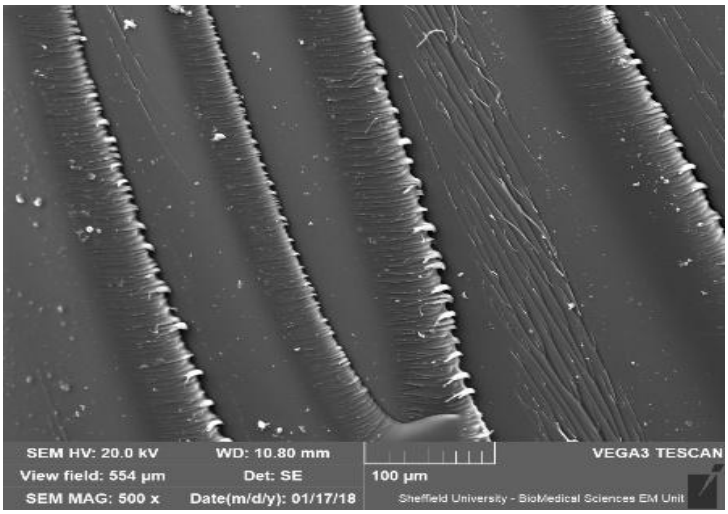

Figure 11 The flexural-fractured surface of the neat Epikote 828

In comparison, both MWCNT_short/828/DDS (Figure 12(a)) and MWCNT_long/828/DDS (Figure 12 (b)) resins were rougher in their respective surface fracture. Incorporating MWCNT into the epoxy resin undoubtedly enhanced the roughness of the fracture surface [41,42]; it was probably the cause for nanocomposites exhibiting further strengthened fracture toughness. Besides, the size and distance of their cleavage planes diminished in contrast to the neat resin that had a ductile failure [43]. Interestingly, the circled area in Figure 12(c) demarcates a zone containing MWCNT from the one that did not. The zone with MWCNT formed a network of cleavage, which was not present in the zone without MWCNT in plain and featureless appearance. Thus, fractography might be useful in measuring the dispersion of CNT in systems with a marked difference in fractures.

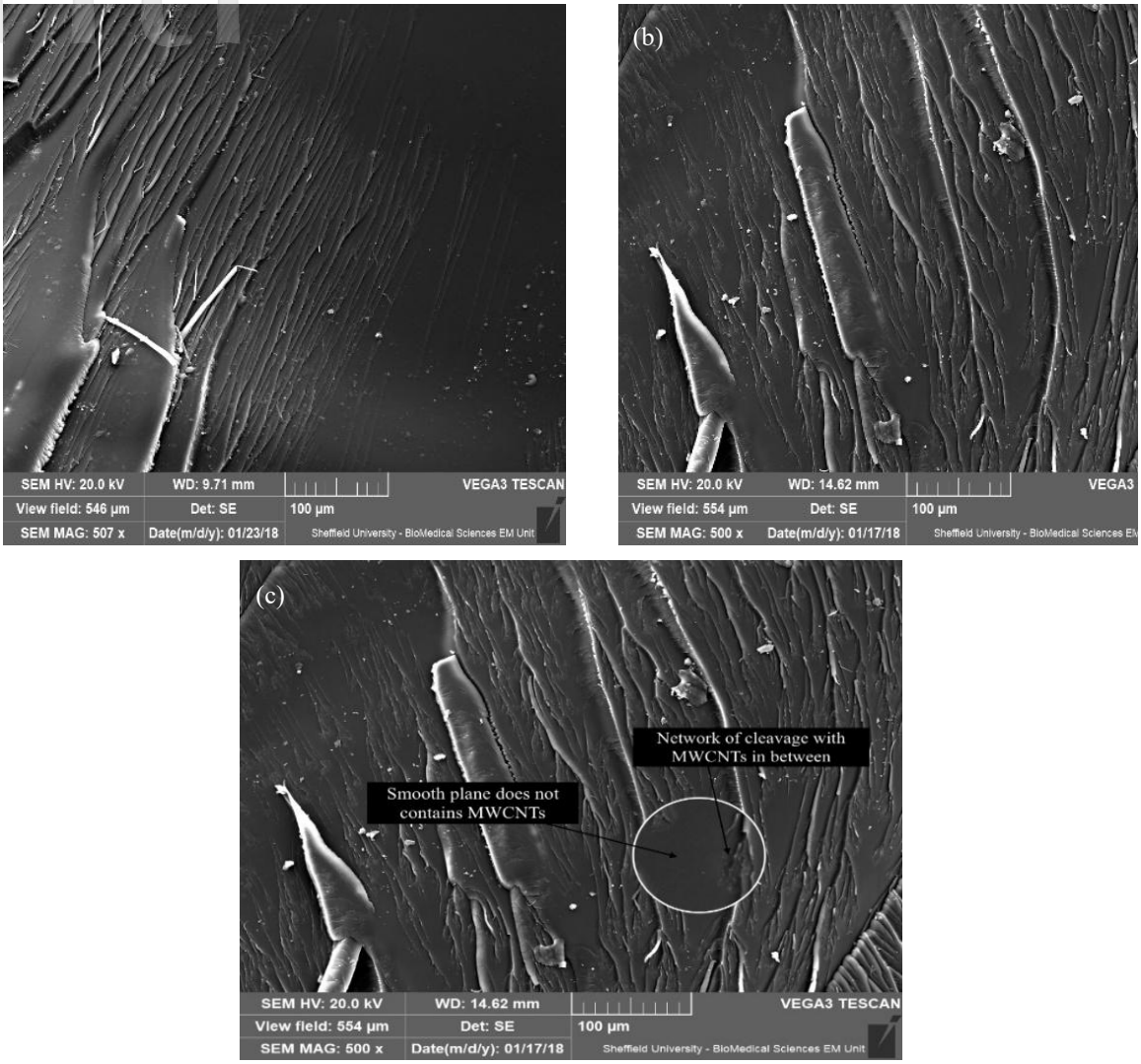

Figure 12 The fractograph of flexural-fractured surface: A) MWCNT_short/828, B) MWCNT_long/828 flexural-fractured surface, and C) magnification of MWCNT_long/828 flexural-fractured surface that distinguished between the zone that was postulated to contain MWCNT and the featureless area without MWCNT

V. CONCLUSIONS

The ILSS of laminated CFRP composites was dependent primarily on the attributes of the matrix [35]. This study enhanced the mechanical attributes of the matrix via the incorporation of MWCNT into it and two types of MWCNT-modified resins were evaluated. The evaluation showed that stiffer resins could be produced using the MWCNT_short composite. The elastic modulus of the Epikote 828 epoxy polymer, estimated in compression and bending, increased by 6.4% with the incorporation of MWCNT. However, for the MWCNT_long resin, the elastic modulus dwindled by 3.1% in contrast to the neat resin. MWCNT improved the flexural toughness of the neat resin. SEM micrographs showed that the creation of micro-cracks and plastic yielding was the principal mechanism of toughening. Meanwhile, the ILSS for MWCNT_short CFRP laminates soared by 14%, while the MWCNT_long CFRP laminates dwindled by 17.4% in ILSS compared to the neat resin CFRP laminates. This is related to the result which was discussed on Raman spectroscopy. The intensity ratio (ID/IG) of the MWCNT_long was higher than MWCNT_short, with the value of 0.68 and 0.39 respectively. This indicates that MWCNT_long contains large quantity of defects of carbon atoms which were bonded with sp2 as compared to the MWCNT_short which decreased the quality of the nano-modified resin although MWCNT long is well dispersed than MWCNT short. The incorporation of MWCNT significantly impacted the ILSS of the CFRP composites (p-value = 3 x 10^{-6}). The nano- and micro-agglomerations in MWCNT_short/828/DDS nanocomposite epoxy matrix might serve as an effective pinning mechanism that prevented the initial cracks from spreading. The mixed techniques of dispersion introduced in this study might be applicable for producing an effective agglomeration for an appropriate pinning mechanism. Also, fractography may be a useful metric for dispersion

in systems showing a marked difference in fractured surfaces.

REFERENCES

[1] Ma PC, et al., "Dispersion and functionalization of carbon nanotubes for polymer-based nanocomposites: A review," *Composites Part A: Applied Science and Manufacturing*, Vol. 41, No. 10, 2010, pp. 1345-1367. https://doi.org/10.1016/j.compositesa.2010.07.003

[2] Thostenson ET, Ren Z, Chou T-W, "Advances in the science and technology of carbon nanotubes and their composites: A review," *Composites Science and Technology*, Vol. 61, No. 13, 2001, pp. 1899-1912. https://doi.org/10.1016/s0266-3538(01)00094-x

[3] Sadykov D, Nouicer L, Lekakou C, "Hybrid Woven Glass Fibre Fabric-Multi-Walled Carbon Nanotube-Epoxy Composites Under Low Rate Impact," *Journal of Composites Science,* Vol. 1, No. 1, 2017. https://doi.org/10.3390/jcs1010010

[4] Visco A, et al., "Cure Rate and Mechanical Properties of a DGEBF Epoxy Resin Modified with Carbon Nanotubes," *Journal of Reinforced Plastics and Composites,* online July 3, 2008. https://doi.org/10.1177/0731684407087560

[5] Popov VN, "Carbon nanotubes: Properties and application," *Materials Science and Engineering: R: Reports*, Vol. 43, No. 3,2004, pp. 61-102. https://doi.org/10.1016/j.mser.2003.10.001

[6] Garg P, et al., "Effect of dispersion conditions on the mechanical properties of multi-walled carbon nanotubes based epoxy resin composites." *Journal of Polymer Research,* Vol. 18, 2010, pp. 1397-1407. https://doi.org/10.1007/s10965-010-9544-8

[7] Song B, et al., "Nanofillers, Significantly Strengthening Epoxy by Incorporating Carbon Nanotubes/Graphitic Carbon Nitride Hybrid," *Macromolecular Materials and Engineering,* Vol. 305, June 2020. https://doi.org/10.1002/mame.202000231

[8] Rogers B, Pennathur S, Adams J, "Nanotechnology: Understanding Small Systems," CRC Press, Taylor and Francis Group: Boca Raton, London, New York, Vol. 47, 2008, pp. 4778-4779. https://doi.org/10.1201/b17424

[9] Bilalis P, et al., "Non-covalent functionalization of carbon nanotubes with polymers," *Royal Society of Chemistry Advances,* Vol. 4, 2014, pp. 2911-2934. https://doi.org/10.1039/c3ra44906h

[10] Rana S, et al., "A Review on Carbon Epoxy Nanocomposites," *Journal of Reinforced Plastics and Composites,* Vol. 28, No. 4, 2008, pp. 461-487. https://doi.org/10.1177/0731684407085417

[11] Song YS, Youn JR, "Influence of dispersion states of carbon nanotubes on physical properties of epoxy nanocomposite," *Carbon,* Vol. 43, Issue 7, 2005, pp. 1378-1385. https://doi.org/10.1016/j.carbon.2005.01.007

[12] Gojny FH, et al., "Carbon nanotube- reinforced epoxy-composites: Enhanced stiffness and fracture toughness at low nanotube content," *Composite Science and Technology,* Vol. 64, 2004, pp. 2363-2371. https://doi.org/10.1016/j.compscitech.2004.04.002

[13] Zhao Z, et al., "Mechanical, thermal and interfacial performances of carbon fiber reinforced composites flavored by carbon nanotube in matrix/interface," *Composite Structures*, Vol. 159, 2017, pp. 761-772. https://doi.org/10.1016/j.compstruct.2016.10.022

[14] Sanchez SR, et al., "Variance Spectroscopy Monitors the Sonication-Induced Cutting and Debundling of Single-Walled Carbon Nanotubes," *ECS Meeting Abstract,* Vol. MA2017-01*,* 2017, p. 697. https://doi.org/10.1149/ma2017-01/9/697

[15] Fu SY, et al., "The reduction of carbon nanotube (CNT) length during the manufacture of CNT/polymer composites and a method to simultaneously determine the resulting CNT and interfacial strengths," *Carbon,* Vol. 47, 2009, pp. 3192-3200. https://doi.org/10.1016/j.carbon.2009.07.028

[16] Russ M, et al., "Length-dependent electrical and thermal properties of carbon nanotube-loaded epoxy nanocomposites," *Composites Science and Technology*, Vol. 81, 2013, pp. 42-47. https://doi.org/10.1016/j.compscitech.2013.03.011

[17] Korayem AH, et al., "Optimizing the degree of carbon nanotube dispersion in a solvent for producing reinforced epoxy matrices," *Powder Technology,* Vol. 284, 2015, pp. 541-550. https://doi.org/10.1016/j.powtec.2015.07.023

[18] Advani SG, Fan Z, "Dispersion, Bonding and Orientation of Carbon Nanotubes in Polymer Matrices," In *Processing and Properties of Nanocomposites*, *World Scientific Publishing Co.Pte. Ltd NJ, USA*, 2007, pp. 61-98. https://doi.org/10.3390/polym4010275

[19] Huang YY, Terentjev EM, "Dispersion of carbon nanotubes: Mixing, sonication, stabilization, and composite properties," *Polymers (Basel),* Vol. 4, 2012, pp. 275-295. https://doi.org/10.3390/polym4010275

[20] Naik RB, et al., "Effect of non-ionic surfactants on thermomechanical properties of epoxy/multiwall carbon nanotubes composites," *Progress in Organics Coatings,* Vol.77, Issue 11, 2014, pp. 1883-1889. https://doi.org/10.1016/j.porgcoat.2014.06.024

[21] Seyhan AT, Tanoğlu M, Schulte K, "Tensile mechanical behavior and fracture toughness of MWCNT and DWCNT modified vinyl-ester/polyester hybrid nanocomposites produced by 3-roll milling," *Material Science and Engineering A,* Vol. 523, Noi. 1-2, 2009, pp. 85-92. https://doi.org/10.1016/j.msea.2009.05.035

[22] Thostenson ET, Chou TW, "Processing-structure-multi-functional property relationship in carbon nanotube/epoxy composites," *Carbon,* Vol. 44, 2006,

pp. 3022-3029.
https://doi.org/10.1016/j.carbon.2006.05.014
[23] Wang Y, Wu J, Wei F, "A treatment method to give separated multi-walled carbon nanotubes with high purity, high crystallization and a large aspect ratio," *Carbon,* Vol. 41, 2003, pp. 2939-2948.
https://doi.org/10.1016/s0008-6223(03)00390-7
[24] Exakt 80E "https://exaktusa.com/pharmacy-equipment/products/exakt-80e/" Available online: https://exaktusa.com/pharmacyequipment/products/exakt-80e/
[25] Martin-Gallego M, et al., Lopez-Manchado MA, "Epoxy Nanocomposites filled with Carbon Nanoparticles," *The Chemical Record,* Vol. 18, No. 7-8, 2018, pp. 928-939.
https://doi.org/10.1002/tcr.201700095
[26] Wu T, Lo T, Kuo W, "Effect of Dispersion on Graphite Nanosheet Composites," *Polymer Composites,* Vol. 31, Issue 2, 2010, pp. 292-298.
https://doi.org/10.1002/pc.20802
[27] Liu W, Chai S, Rahman A, Hashim U, "Journal of Industrial and Engineering Chemistry Synthesis and characterization of graphene and carbon nanotubes: A review on the past and recent developments," *Journal of Industrial and Engineering Chemistry*, Vol. 20, 2014, pp. 1171-1185.
https://doi.org/10.1016/j.jiec.2013.08.028
[28] Zakaria MR, et al., "Comparative study of graphene nanoparticle and multiwall carbon nanotube filled epoxy nanocomposites based on mechanical, thermal and dielectric properties," *Composite Part B Engineering,* Vol. 119, 2017, pp. 57-66.
https://doi.org/10.1016/j.compositesb.2017.03.023
[29] Tuinstra F, Koenig JL, "Raman Spectrum of Graphite," *Journal of Chemical Physics,* Vol. 53, 1970, pp. 1126-1130.
https://doi.org/10.1016/j.compositesb.2017.03.023
[30] Osswald S, Havel M, Gogotsi Y, "Monitoring oxidation of multiwalled carbon nanotubes by Raman spectroscopy," *Journal of Raman Spectroscopy,* Vol. 38, 2007, pp. 728-736.
https://doi.org/10.1002/jrs.1686
[31] British Standard BS EN ISO 604:2003 "Plastics — Determination of compressive properties," Vol. 3, 2003.
https://knowledge.bsigroup.com/products/plastics-determination-of-compressive-properties
[32] ASTM ASTM D695 - 02a "Standard Test Method for Compressive Properties of Rigid Plastics," 2002.
https://store.astm.org/d0695-02a.html
[33] Bruno Faria, Cátia Guarda, Nuno Silvestre, José NC, Lopes DG, "Strength and failure mechanisms of cnt-reinforced copper nanocomposite," *Composites Part B Engineering,* Vol. 145, 2018, pp. 108-120.
https://doi.org/10.1016/j.compositesb.2018.02.033
[34] ASTM D 2344/D 2344M "Standard Test Method for Short-Beam Strength of Polymer Matrix Composite Materials and Their Laminates," 2000.
https://store.astm.org/d2344_d2344m-00e01.html
[35] Fan Z, Santare MH, Advani SG, "Interlaminar shear strength of glass fiber reinforced epoxy composites enhanced with multi-walled carbon nanotubes," *Composites Part A Applied Science Manufacturing,* Vol. 39, 2008, pp. 540-554.
https://doi.org/10.1016/j.compositesa.2007.11.013
[36] Abali F, Pora A, Shivakumar K, "Modified short beam shear test for measuring interlaminar shear strength of composites". *Journal of Composites Material,* Vol. 37, 2003, pp. 453-464.
https://doi.org/10.1177/0021998303037005053
[37] Shindo Y, Wang R, Horiguchi K, "Analytical and Experimental Studies of Short-Beam Interlaminar Shear Strength of G-10CR Glass-Cloth/Epoxy Laminates at Cryogenic Temperatures," *Journal of Engineering Materials and Technology,* Vol. 123, 2001, pp. 112.
https://doi.org/10.1115/1.1286235
[38] Cui WC, Wisnom MR, "Contact finite element analysis of three- and four-point short- beam bending of unidirectional composites," *Composites Science and Technology,* Vol. 45, 1992, pp. 323-334.
https://doi.org/10.1016/0266-3538(92)90047-7
[39] Gürkan I, Cebeci H, "An approach to identify complex CNT reinforcement effect on the interlaminar shear strength of prepreg composites by Taguchi method," *Composite Structure,* Vol. 141, 2016, pp. 172-178.
https://doi.org/10.1016/j.compstruct.2016.01.043
[40] Andrew Rutherford, Daniel B, "Introducing ANOVA and ANCOVA: a GLM approach (introducing statistical methods series)," Editor Daniel B.W, Sage Publications, Edition 1st, 2001.
https://in.sagepub.com/en-in/ind/introducing-anova-and-ancova/book205673
[41] Hosur M, et al., "Effect of processing techniques on the performance of Epoxy/MWCNT nanocomposites," *Journal of Applied Polymer Science,* Vol. 127, 2013, pp. 4211-4224.
https://doi.org/10.1002/app.37990
[42] Zhou Y, et al., "Fabrication and characterization of carbon/epoxy composites mixed with multi-walled carbon nanotubes". *Material Science Engineering A*, Vol. 475, 2008, pp. 157-165.
https://doi.org/10.1016/j.msea.2007.04.043
[43] Singh S, Srivastava V.K, Prakash R, "Characterisation of multi-walled carbon nanotube reinforced epoxy resin composites," *Material Science* Technology, Vol. 29, 2013, pp. 1130-1134.
https://doi.org/10.1179/1743284713y.0000000288
[44] Barra G, et al., "Different methods of dispersing carbon nanotubes in epoxy resin and initial evaluation of the obtained nanocomposite as a matrix of carbon fiber reinforced laminate in terms of vibroacoustic performance and flammability," *Materials*, Vol. 12, No. 18, 2019, Article No. 2998.
https://www.mdpi.com/1996-1944/12/18/2998